



Research Article

The Nuclear-Encoded Cytochrome c Oxidase Subunit COX4-1 Enhances Hypoxia Tolerance in Glioblastoma Cells

Claudia R. Oliva^{1*}, Susanne Flor¹, Md Yousuf Ali², Corinne E. Griguer^{1*}

¹Free Radical & Radiation Biology Program, Department of Radiation Oncology, The University of Iowa, Iowa City, IA, 52242, USA.

²Mass General Hospital Center for Cancer Research, Harvard Medical School, Boston, MA, 02129, USA.

***Corresponding author:** Oliva CR and Griguer CE, Free Radical & Radiation Biology Program, Department of Radiation Oncology, The University of Iowa, Iowa City, IA, 52242, USA.

Citation: Oliva CR, Flor S, Ali MY, Griguer CE (2025) The Nuclear-Encoded Cytochrome c Oxidase Subunit COX4-1 Enhances Hypoxia Tolerance in Glioblastoma Cells. J Oncol Res Ther 10: 10299. DOI: 10.29011/2574-710X.10299.

Received Date: 8 August, 2025; **Accepted:** 18 August, 2025; **Published Date:** 21 August, 2025.

Abstract

Glioblastoma (GBM) is the most common and aggressive primary brain cancer in adults. While chemo- and radiotherapy are often effective in treating newly diagnosed GBM, increasing evidence suggests that treatment-induced metabolic alterations promote tumor recurrence and further resistance. In addition, GBM tumors are typically hypoxic, which further contributes to treatment resistance. Recent studies have shown that changes in glioma cell metabolism driven by a shift in the isoform expression of mitochondrial cytochrome c oxidase (CcO) subunit 4 (COX4), a key regulatory subunit of mammalian CcO, may underlie the treatment-induced metabolic alterations in GBM cells. However, the impact of hypoxia on GBM energetics is not fully understood. Using isogenic GBM cell lines expressing either COX4-1 or the alternative COX4 isoform, COX4-2, we found that COX4-1 expressing cells maintained a more oxidative metabolism under hypoxia, characterized by increased CcO activity and ATP production, enhanced assembly of CcO-containing mitochondrial supercomplexes, and reduced superoxide production. Furthermore, COX4-1 expression was sufficient to increase radioresistance under hypoxic conditions. Untargeted metabolomic analysis revealed that the most significantly upregulated pathways in COX4-1-expressing cells under hypoxia were purine and methionine metabolism. In contrast, COX4-2-expressing cells showed increased activation of glycolysis and the Warburg effect. Our study provides new insights into how CcO regulatory subunits influence cellular metabolic networks and radioresistance in GBM under hypoxia, identifying potential therapeutic targets for improved treatment strategies.

Abbreviations:

CcO, cytochrome c oxidase

ETC, electron transport chain

OXPPOS, oxidative phosphorylation

SCs, mitochondrial supercomplexes

OCR, mitochondrial oxygen consumption rate

ROS, reactive oxygen species

O₂^{-•}, superoxide

ATP, Adenosine triphosphate

PRPP, phosphoribosyl pyrophosphate

IMP, inosine monophosphate

XMP, xanthosine 5'-monophosphate

5'AMP, 5' adenosine monophosphate

GBM, glioblastoma.

Keywords: Cytochrome c oxidase; Glioma; Hypoxia; COX4-1; Mitochondrial supercomplexes; Radioresistance.

Introduction

GBM is a highly aggressive cancer that almost invariably recurs,

largely due resistance of some GBM cells to standard therapy, including chemotherapy and radiotherapy [1-4]. Within GBM tumors, the median partial pressure of oxygen is reported to be between 5-9 mm Hg (~0.65% to 1.18% O₂), and this hypoxic environment is linked to tumor growth and resistance to both chemotherapy and radiation therapy due to the lack of the oxygen enhancement effect [5, 7]. Consequently, identifying the molecular mechanisms that exacerbate the tumor-supporting effects of hypoxia may aid in developing more effective therapeutic options for GBM. Recent studies have revealed that cytochrome c oxidase (CcO) plays a significant role in regulating tumorigenesis and treatment responses across various cancer types [8-11], including GBM, but the molecular mechanisms underlying these tumor regulating processes remain poorly understood.

CcO is the terminal enzyme of the electron transport chain (ETC) and thus critically regulates oxidative phosphorylation (OXPHOS) and ATP generation. Mammalian CcO comprises 13 subunits, of which three (COX1-3) are encoded by mitochondrial DNA. The remaining ten subunits are encoded by nuclear genes and are imported into different mitochondrial compartments to assist in CcO complex assembly [12-14]. Research by us and others has shown that the expression of specific isoforms of these regulatory CcO subunits is associated with aggressive tumor behavior and resistance to apoptosis in breast carcinoma cells (COX7AR), lung adenocarcinoma cells (COX6B2), and GBM cells (COX4-1) [8-10, 15, 16].

Under physiologic conditions, COX4 controls the enzymatic activity of CcO in response to cellular ATP concentrations, enhancing CcO activity and, consequently, OXPHOS when ATP levels are low [17]. Two isoforms of COX4, COX4-1 and COX4-2, are found in mammals [12, 13]. COX4-1 expression is necessary for coupling ATP production to cellular energy demands, a process that is directly regulated by the allosteric binding of ATP to COX4-1. In contrast, COX4-2 lacks the serine 58 residue that regulates ATP binding and contains three cysteine residues that likely function as redox sensors [18, 19]. Our research also revealed that treatment of glioma cells with ionizing radiation triggers a switch from high COX4-2 and low or no COX4-1 expression to high COX4-1 and low or no COX4-2 expression. This switch from COX4-2 to COX4-1 expression leads to an OXPHOS phenotype, a reduction in superoxide (O₂^{•-}) levels, and the development of resistance to both radio- and chemotherapy under normoxic conditions [9, 16].

Considering the hypoxic conditions within GBM tumors, the reliance on the oxygen-consuming OXPHOS pathway in therapy-resistant GBM cells may seem paradoxical, and the mechanisms facilitating this effect remain largely unknown. However, our research further showed that COX4-1 expression in glioma cells drives the assembly of individual ETC complexes

into mitochondrial supercomplexes (SCs) [9]. The presence of mitochondrial SCs has been shown to enhance ETC efficiency, and recent research suggests that the assembly of such SCs is vital for the survival of pancreatic, breast, and endometrial cancer cells under severe hypoxia [8, 10, 20].

In this study, we explored the role of mitochondrial respiration and SC assembly in the radioresistance of glioma cells under low-oxygen conditions, using an untargeted metabolomic profiling platform to quantify biochemical differences in glioma cells developed in our prior studies to overexpress the COX4 isoforms [9, 15, 16, 21].

Materials and Methods

Glioma cell lines

The generation of COX4-1- and COX4-2-overexpressing U251 cells was previously described [9, 15, 21]. Cells were grown in DMEM F-12, L-glutamine and 7% FBS. Hypoxia was induced by placing the cells in a BioSpherix hypoxia chamber (Parish, NY) with a humidified atmosphere containing 1% O₂ for 24-48 hours.

Mitochondrial isolation and assays

Mitochondrial fractions were prepared from cultured cells as we previously described [9, 15, 16]. Briefly, cells pellets were resuspended in buffer (10 mM NaCl, 1.5 mM MgCl₂, and 10 mM Tris-HCl, pH 7.5) and then disrupted with a Dounce glass homogenizer. The homogenate was then centrifuged at 1000 × g for 10 min, and the resulting supernatant was further centrifuged at 20,000 × g for 20 min. Mitochondria were solubilized in 10 mM potassium phosphate buffer supplemented with 0.2% n-dodecyl β-D-maltoside. The mitochondrial oxygen consumption rate (OCR) was measured after the induction of state 3 respiration. Mitochondrial complex activities were determined as previously described [9, 15, 16]. For blue native polyacrylamide gel electrophoresis (BN-PAGE), mitochondrial pellets were solubilized in NativePAGE Sample Buffer (4X; Invitrogen, catalog # BN20032) containing digitonin (Invitrogen, catalog # BN2006) at a digitonin/protein ratio of 4 g/g. Samples were separated on 3–12% NativePAGE Bis-Tris gels (Invitrogen, catalog # BN2012BX10) [9].

Mitochondrial superoxide determination

Intracellular ROS production was determined by measuring the levels of O₂^{•-} produced in the cells by flow cytometry after staining the cells with MitoSOX™ Red (Invitrogen, Carlsbad, CA) as previously described [9, 22]. Briefly, cells were plated in six well plates and then exposed to 1% O₂ for varying time periods. Cells were further incubated with MitoSOX™ Red (2 μM) for 25 min. Fluorescence was analyzed by flow cytometry (510 nm excitation and 580 nm emission). A total of 10,000 events were obtained per sample. The data were then analyzed using FlowJo v10 software.

2.4 Cell proliferation assay To assess cell proliferation, cells were seeded into 6-well plates. Cell number was assayed every 24 hours for 5 days using a TC20 automated cell counter (BioRad, Hercules, CA) as we previously described [23].

Clonogenic survival assays

To assess cell survival after ionizing radiation, cells were plated in 60-mm dishes and 2, 4, 6, or 8 Gy was then delivered to the cells, with a dose rate of 0.805 Gy/min, using a 6000 Ci137Cs cesium irradiator (J.L. Shepherd, San Fernando, CA). Cells were then plated at low density and clones were allowed to grow under normoxia or 1% O₂ for 10–14 days, then were fixed with 70% ethanol and stained with Coomassie blue for analysis of clonogenic survival [9, 24].

Metabolomic analysis

Sample preparation and metabolomic analysis was performed as previously described [21].

Xenograft Mouse Model with Intracranial Tumors

All animal experiments and surgical procedures were conducted with approval from the Institutional Animal Care and Use Committee of the University of Iowa. Six-week-old female athymic nude mice were obtained from Envigo (Indianapolis, IN) and randomly divided into two groups of five. A total of 3×10^5 of COX4-1 and COX4-2-expressing cells suspended in 5% methylcellulose, were injected intracranially as previously described [15, 23]. The primary endpoint of the study was animal survival; moribund animals that became unresponsive to mild external stimuli were euthanized, and this date was recorded as the estimated date of death.

Statistics Analysis

All data were evaluated using GraphPad Prism (GraphPad Software, San Diego, CA). Results are expressed as the mean \pm SD, and $p < 0.05$ was considered significant. Statistical analyses were performed using two-way analysis of variance (ANOVA), followed by Tukey's multiple comparison test or (un)paired Student t test. Statistical significance was indicated with asterisks: * $p < 0.05$, ** $p < 0.01$, *** $p < 0.001$ and **** $p < 0.0001$.

Results

COX4-1 expression promotes oxidative metabolism in glioma cells under hypoxia

Cytochrome c oxidase subunit 4 (COX4) is a key regulatory subunit of CcO, and recent studies have demonstrated that COX4 isoform 1 (COX4-1) could have a role in glioma chemo- and radioresistance [9, 15, 16].

To determine the metabolic effects of glioma cell COX4 isoform expression in hypoxic conditions, we assessed the metabolic phenotypes of COX4-1- and COX4-2-expressing GBM cells, first determining the mitochondrial oxygen consumption rate (OCR) to reflect mitochondrial OXPHOS activity. In mitochondria isolated from cells maintained under normoxia or exposed to hypoxia (1% O₂) for 24–48 hours, respiration was induced by the addition of glutamate and malate to activate complex I or succinate to activate complex II, and state 3 (OXPHOS) respiration was induced by the subsequent addition of ADP.

Under normoxia, the OCR was significantly higher in the mitochondria from COX4-1 expressing cells than in the mitochondria from the isogenic COX4-2 lines, regardless of the substrate (Fig. 1A). In addition, COX4-1 expression largely prevented the hypoxia-induced reduction in state 3 respiration observed with COX4-2 expression (Fig. 1A). To determine the maximal mitochondrial uncoupled respiration rate (reserve capacity [RC]), carbonyl cyanide p-trifluoromethoxy-phenylhydrazone (FCCP) was added sequentially at increasing concentrations, and maximal uncoupled respiration was determined at 1.0 μ M FCCP. Under normoxia, the RC was also significantly higher in the mitochondria from the COX4-1-expressing cells than in the mitochondria of the COX4-2-expressing cells (Fig. 1B). Furthermore, COX4-1 expression largely prevented the hypoxia-induced reduction in RC observed in COX4-2-expressing cells (Fig. 1B).

In the OXPHOS phenotype, higher OCR is linked to higher cellular energy (ATP) production [25, 26]. To further confirm that COX4-1 expression is associated with an OXPHOS phenotype rather than a glycolytic phenotype under hypoxia, we examined the rate of ATP production and assessed the rate of glucose uptake and lactate production to reflect glycolytic activity in each cell line. Under normoxia, COX4-1- and COX4-2-expressing cells had similar levels of ATP production. However, COX4-1 expression led to a higher rate of ATP production under hypoxia (Fig. 2A). In contrast to OCR, cellular glucose consumption and lactate production were higher in the COX4-2 cells under normoxia (Fig. 2B-C). Furthermore, COX4-1 expression largely prevented the hypoxia-induced increase in glucose uptake and lactate production observed in COX4-2-expressing cells. These results indicate that expression of COX4-1 in GBM cells is associated with OXPHOS under hypoxic conditions.

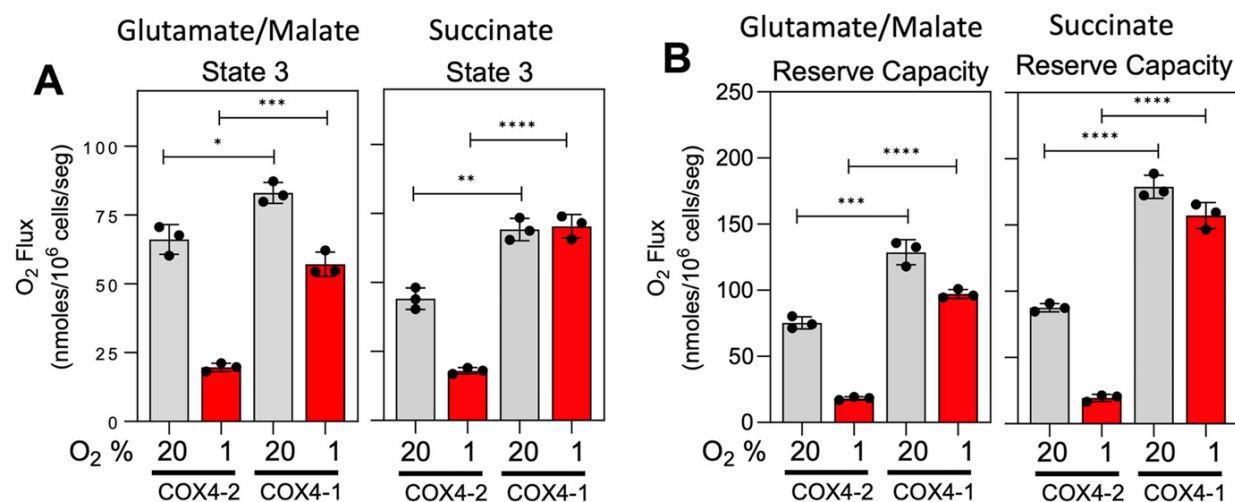


Figure 1: COX4-1-expressing glioma cells maintain higher mitochondrial respiration under hypoxia. OCR (A) and RC (B) in glutamate/malate-dependent and succinate-dependent state 3 respiration induced in mitochondria isolated from COX4-1- and COX4-2-expressing cells cultured under normoxia (gray bars) or hypoxia (red bars) for 24 hours. Data are presented as the mean \pm SEM of three independent experiments. *, $p < 0.05$; **, $p < 0.01$; ***, $p < 0.001$; ****, $p < 0.0001$.

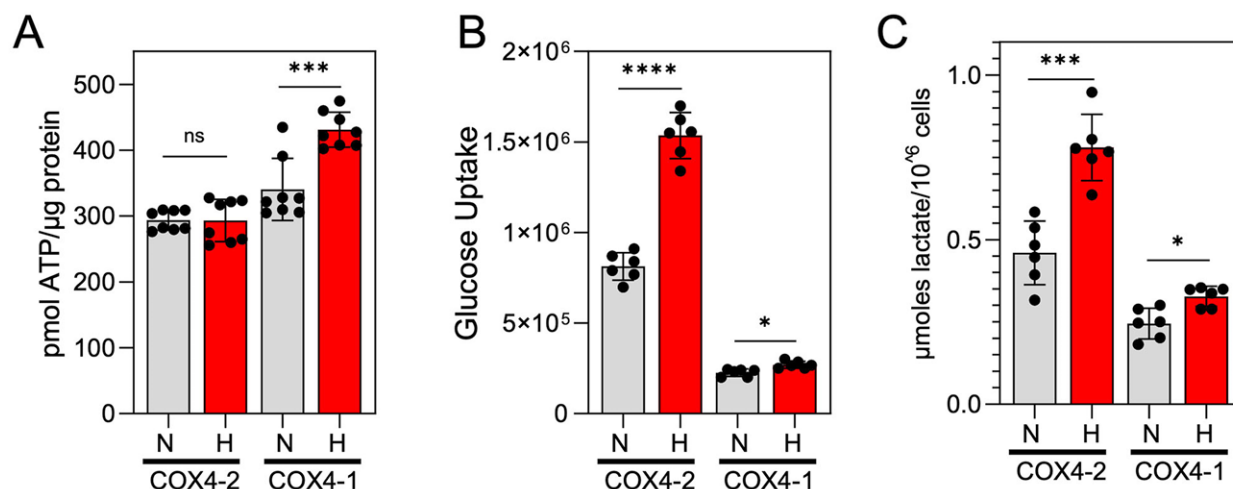


Figure 2: COX4-1-expressing glioma cells maintain an OXPHOS phenotype under hypoxia. (A) Quantification of the ATP production rate in COX4-1- and COX4-2-expressing cells cultured under normoxia (gray bars) or hypoxia for 24 hours (red bars). Data are presented as the mean \pm SEM of three independent experiments. (B) Quantification of cellular glucose uptake, estimated with the non-phosphorylatable fluorescent glucose analogue 2-NBDG, in COX4-1- and COX4-2 expressing cells cultured under normoxia (gray bars) or hypoxia (red bars) for 24 hours. Data are presented as the mean \pm SEM of three independent experiments. (C) Quantification of extracellular lactate concentrations in COX4-1 and COX4-2 cells cultured under normoxia (gray bars) or hypoxia (red bars) for 24 hours. Data are presented as the mean \pm SEM of three independent experiments. *, $p < 0.05$; ***, $p < 0.001$; ****, $p < 0.0001$; N, normoxia; H, hypoxia.

COX4-1 promotes changes in ETC complex activities and $O_2^{\cdot -}$ production in glioma cells under hypoxia

Under normoxia, the activity of complex I and complexes II-III were higher in COX4-1-expressing cells than in COX4-2 expressing cells. Hypoxia exposure increased complex I activity in COX4-2-expressing cells but did not further increase the activity in COX4-1-expressing cells (Fig. 3A). Hypoxia exposure also increased the activity of complexes II-III in COX4-2-expressing cells, but did not further increase the activity in COX4-1-expressing cells (Fig. 3B). Under normoxia, COX4-1 expression also led to greater CcO activity than COX4-2 expression did, as we previously described [15, 16]. In contrast to the effects of hypoxia on complexes I and II-III, hypoxia exposure further reduced the activity of CcO in

COX4-2-expressing cells. (Fig. 3C). However, hypoxia did not cause a significant change in CcO activity in COX4-1-expressing cells (Fig. 3C).

We next used the mitochondria-targeted probe MitoSOX to determine $O_2^{\cdot -}$ production in the intact COX4-1- and COX4-2-expressing cells exposed to hypoxia. In agreement with the observation that hypoxia increased the activity of complexes I and II-III in COX4-2-expressing cells, hypoxia also increased $O_2^{\cdot -}$ production in these cells (Fig. 3D). Despite the relatively high activity of each ETC complex detected in COX4-1-expressing cells, however, $O_2^{\cdot -}$ production in these cells was approximately 3-fold lower than that in COX4-2-expressing cells under normoxia and was comparable with pre-hypoxia levels. (Fig. 3D).

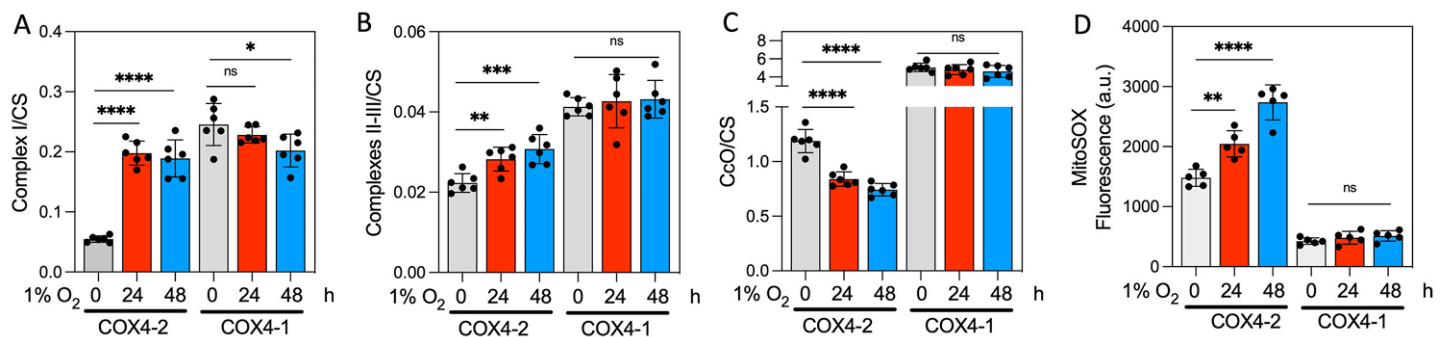


Figure 3: COX4-1 cells maintain mitochondrial function under hypoxia. Relative activities of (A) complex I, (B) complexes II-III, and (C) CcO activity, normalized to citrate synthase (CS) activity from COX4-1 and COX4-2 cells exposed to hypoxia are shown. (D) Quantification of mitochondrial $O_2^{\cdot -}$ production in COX4-1 and COX4-2 cells under normoxia and hypoxia. Columns represent the average from triplicate determinations from at least two independent experiments. $p < 0.05$ (*), $p < 0.01$ (**), $p < 0.001$ (***), and $p < 0.0001$ (****).

Because we previously demonstrated that overexpression of COX4-1 in glioma cells was sufficient to promote the incorporation of CcO into SCs under normoxia [9], we investigated whether COX4-1-expressing cells maintain SCs assembly during hypoxia. Mitochondria were prepared from the COX4-1 cells cultured in normoxic or hypoxic conditions and analyzed by BN-PAGE with

subsequent IGA and western blot. Under normoxia, only a small fraction of CI was present as a free complex in COX4-1-expressing mitochondria, whereas the rest was found in SCs that contained CI, CIII, and CIV at varying ratios (Fig. 4). We have previously demonstrated that cells expressing only the COX4-2 isoform do not assemble mitochondrial complexes into SCs [9].

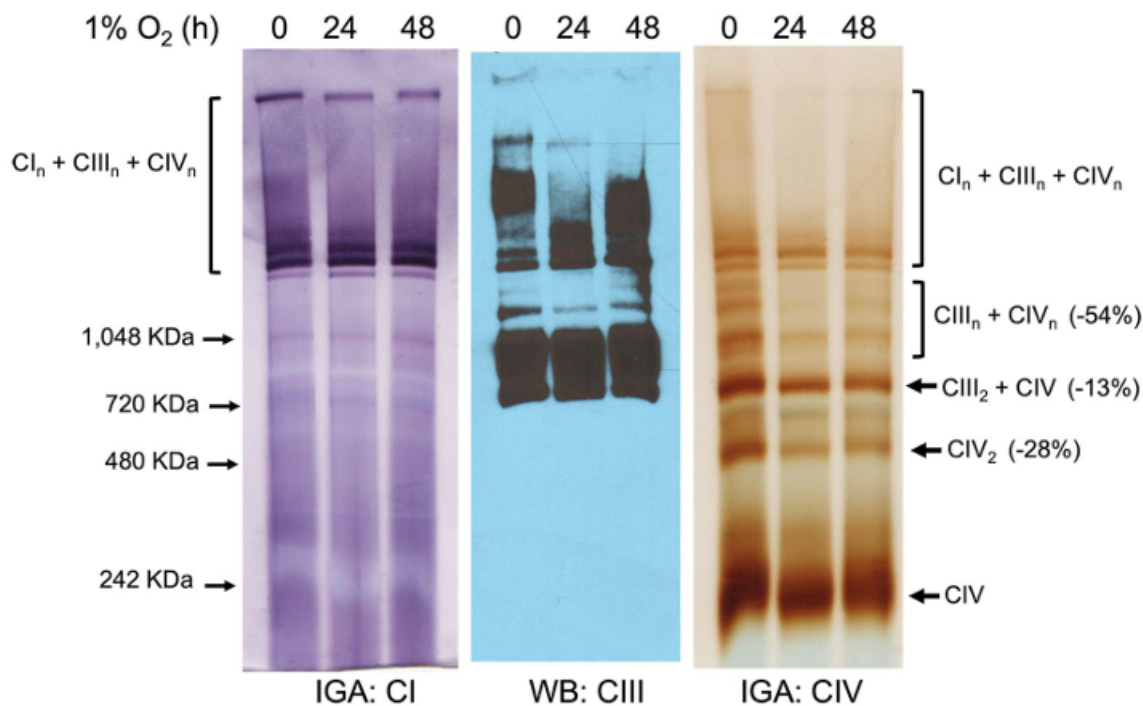


Figure 4: COX4-1-expressing glioma cells maintain SC assembly under hypoxia. Digitonin solubilized mitochondria from COX4-1-expressing cells cultured under normoxia or hypoxia for 24-48 hours were subjected to BN-PAGE followed by IGA to detect complex I and IV activity and Western blot for complex III. Representative images from three separate experiments are shown.

COX4-1 promotes cell proliferation and radioresistance in glioma cells under hypoxia

We next determined if the COX4-1-related changes in cellular energetics correlated with changes in cell proliferation under hypoxia. Compared with COX4-2-expressing cells, COX4-1 expressing cells had a significantly faster proliferation rate under hypoxia in vitro (doubling time: 32.75 ± 2.87 h vs 13.58 ± 1.21 ,

respectively; Fig. 5A). To further determine whether this effect occurred in vivo, we orthotopically implanted COX4-1-expressing or COX4-2-expressing glioma cells into the brains of nude mice. Mice inoculated with COX4-1-expressing tumor cells had a median survival of only 22 days. In contrast, all mice inoculated with COX4-2-expressing cells remained alive at the end of the study (60 days) (Fig. 5B).

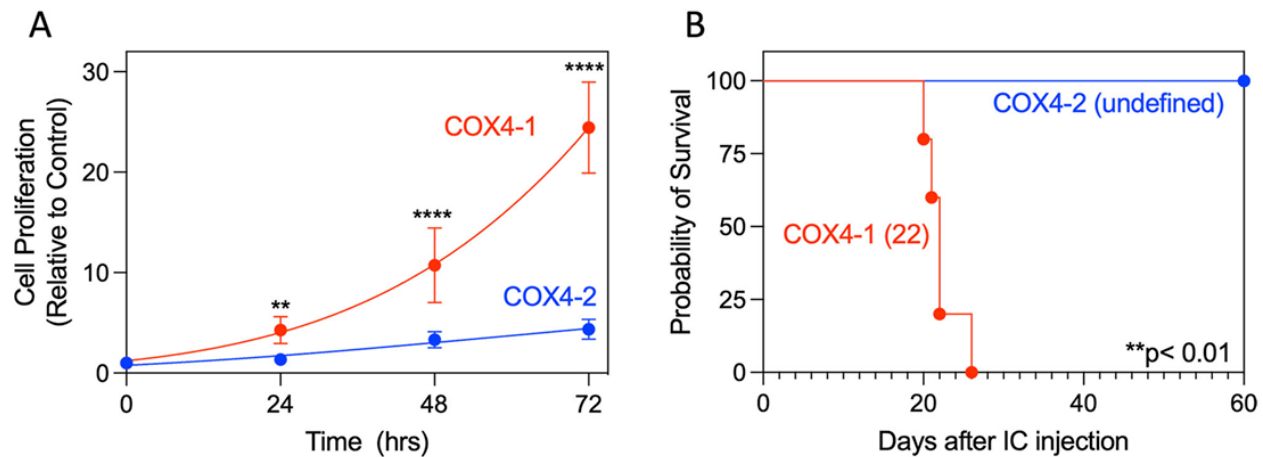


Figure 5: COX4-1-expressing glioma cells maintain a high proliferation rate under hypoxia. **(A)** Quantitative analysis of cell proliferation over time under hypoxia in adherent cultures of COX4-1-expressing and COX4-2-expressing cells (n=6). ** p<0.01; and **** p<0.0001, by two-way ANOVA. **(B)** Kaplan-Meier survival curves of overall survival in nude mice harboring orthotopic brain tumors generated by inoculation with glioma cells expressing COX4-1 (n=5) or COX4-2 (n=5). The log-rank test yielded a p-value of <0.01, and the fraction of survival is expressed with a 95% confidence interval (CI) using the asymmetrical method.

To investigate whether COX4-1-expressing cells maintain the radioresistant phenotype [9, 24] with secondary irradiation, we tested cell viability in response to varying amounts of single-dose irradiation using a clonogenic assay, which is considered a gold standard for assessing the long-term effects of radiation [27]. Cells were exposed to 2, 4, 6, and 8 Gy under normoxia or hypoxia, and colony-forming ability was measured after 14 days. Under normoxia, COX4-1 cells exhibited greater resistance to radiation than COX4-2 cells did. Significantly, hypoxia further enhanced the resistance to radiation of COX4-1-expressing cells relative to that of COX4-2-expressing cells (Fig. 6).

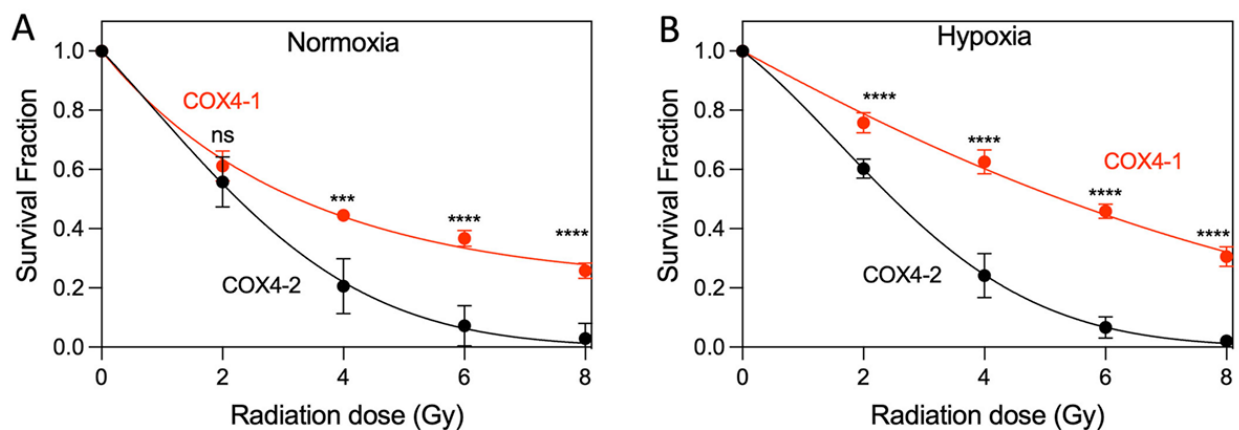


Figure 6: COX4-1 cells exhibit increased radioresistance under hypoxia. Clonogenic survival curves for COX4-1 and COX4-2-overexpressing cells under **(A)** normoxia, and **(B)** hypoxia. Cells were irradiated with 2, 4, 6, or 8 Gy and immediately plated. Clonogenic survival was estimated on day 14 after irradiation. p < 0.001 (***) and p < 0.0001 (****), calculated using two-way ANOVA followed by Tukey's multiple comparison test.

COX4-1 promotes alterations in purine and methionine metabolism in glioma cells under hypoxia

To understand the global metabolomic changes related to hypoxia exposure, untargeted metabolomic analysis was performed on COX4-1-expressing and COX4-2-expressing cells exposed to 1% O₂ for 24 hours (Fig. 7). Using an integrated metabolomics platform [21], we identified 519 compounds of known identity (biochemicals) in the COX4-1- or COX4-2-expressing cells exposed to hypoxia. Analysis by two-way ANOVA identified 364 biochemicals that achieved statistical significance ($p \leq 0.05$) and exhibited significant interaction and main effects for experimental parameters of genotype. Among those biochemicals, 208 biochemicals were upregulated and 156 biochemicals were downregulated in the COX4-1-expressing cells compared with

the levels in COX4-2-expressing cells. To identify the metabolites driving the distinction between the two isoform-overexpressing cells, we performed an ANOVA to compare the relative levels of individual metabolites and altered common pathways in each. The two most significantly upregulated pathways associated with COX41 expression under hypoxia were purine and methionine metabolism (Fig. 7B); the two most significantly upregulated metabolic pathways associated with COX4-2 expression under hypoxia were glycolysis and Warburg effect (Fig. 7C). These findings indicate that changes in the glioma cell metabolome under hypoxia correlate with a change in the COX4 isoform expressed, prompting us to further examine the effect of COX4 isoform expression on the metabolites involved in these pathways.

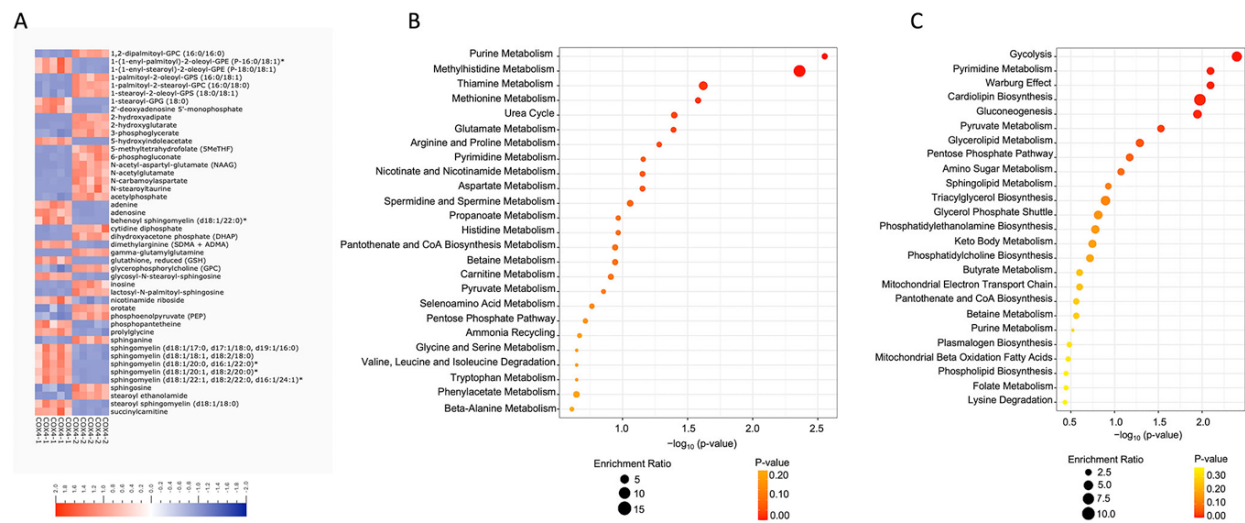


Figure 7: Comparison of metabolomic profiles of COX4-1 and COX4-2 cells under hypoxia. (A) Heatmap of the top 100 altered metabolites in COX4-1 and COX4-2 cells under hypoxia. Blue indicates decreased value and red indicates increased value of each compound listed. Pathway enrichment analysis of (B) COX4-1 and (C) COX4-2 cells under hypoxia.

Metabolic pathway analysis in glioma cells overexpressing COX4 isoforms under hypoxia

Under hypoxia, the levels of metabolites involved in the de novo synthesis of purines were upregulated in the COX4-1-expressing cells relative to levels in the COX4-2-expressing cells. Specifically, phosphoribosyl pyrophosphate (PRPP), inosine monophosphate (IMP), xanthosine 5'monophosphate (XMP), and 5'AMP were 1.5-fold, 4.0-fold, 1.4-fold higher, and 5.0-fold higher, respectively, in

COX4-1-expressing cells. Additionally, the level of adenosine and adenine metabolites involved in the purine salvage pathway were 18-fold and 30-fold higher, respectively, in the COX41-expressing cells (Fig. 8). Interestingly, the levels of some metabolites involved in the purine degradation pathway were upregulated in the COX4-2-expressing cells, including the levels of hypoxanthine (65-fold) and inosine (30-fold) (Fig. 8).

Figure 8

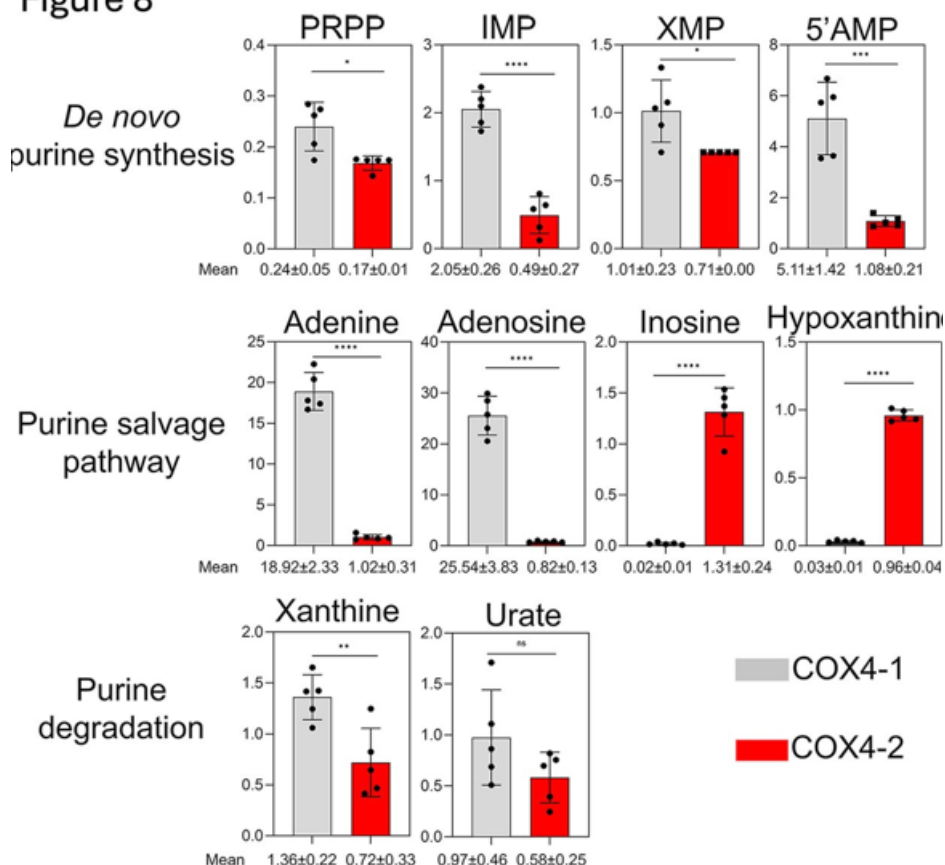


Figure 8: Effects of COX4-1 and COX4-2 expression on purine cycle metabolites in glioma cells under hypoxia. Bars represent the levels of key metabolites involved in the purine pathway analyzed in COX4-1-expressing (gray bars) and COX4-2-expressing (red bars) glioma cells cultured under hypoxia for 24 hours. The numbers below each graph indicate the mean value ± SD for each metabolite, based on five independent measurements. *, $p < 0.05$; **, $p < 0.01$; ***, $p < 0.001$; ****, $p < 0.0001$; ns, not significant; PRPP, phosphoribosyl pyrophosphate; IMP, inosine monophosphate; XMP, xanthosine 5'-monophosphate.

Levels of metabolites associated with the transmethylation and transsulfuration pathways were also significantly upregulated in the COX4-1-expressing cells relative to levels in the COX4-2-expressing cells under hypoxia. Levels of methionine,

S-adenosylmethionine, and S-adenosylhomocysteine were 2-fold, 17-fold, and 4-fold higher, respectively, and levels of cystathione, cysteine, hypotaurine, and taurine were 3.0-fold, 1.3-fold, 3-fold, and 2.5-fold higher in the COX4-1-expressing cells (Fig. 9).

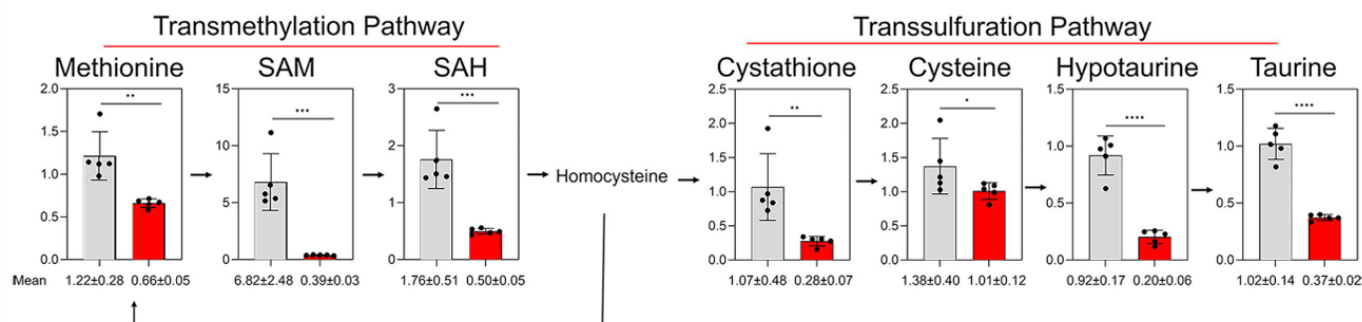


Figure 9: Effects of COX4 isoform expression on methionine pathway metabolites in glioma cells exposed to hypoxia. Bars represent the levels of key metabolites involved in the methionine pathway analyzed in COX4-1-expressing (gray bars) and COX4-2-expressing (red bars) glioma cells cultured under hypoxia for 24 hours. The numbers below each graph indicate the mean value ± SD for each metabolite, based on five independent measurements. *, $p < 0.05$; **, $p < 0.01$; ***, $p < 0.001$; ****, $p < 0.0001$.

In contrast, the levels of most glycolysis pathway metabolites were lower in the COX4-1-expressing cells relative to those in the COX4-2-expressing cells under hypoxia. Levels of glucose, glucose-6-phosphate, fructose 6-phosphate, glyceraldehyde 3-phosphate, dihydroxyacetone phosphate, 3-phosphoglycerate, and phosphoenolpyruvate were, respectively, 1.6-fold, 8-fold, 20-fold, 1.4-fold, 32-fold, 5-fold, and 3.5-fold lower in the COX4-1-expressing cells. Although pyruvate levels were not greatly influenced by the COX4 isoform expressed, lactate levels were also 2.3-fold lower in the COX4-1-expressing cells (Fig. 10). These findings indicate the molecular mechanisms by which COX4-1 expression enhances glioma cell survival in hypoxic conditions.

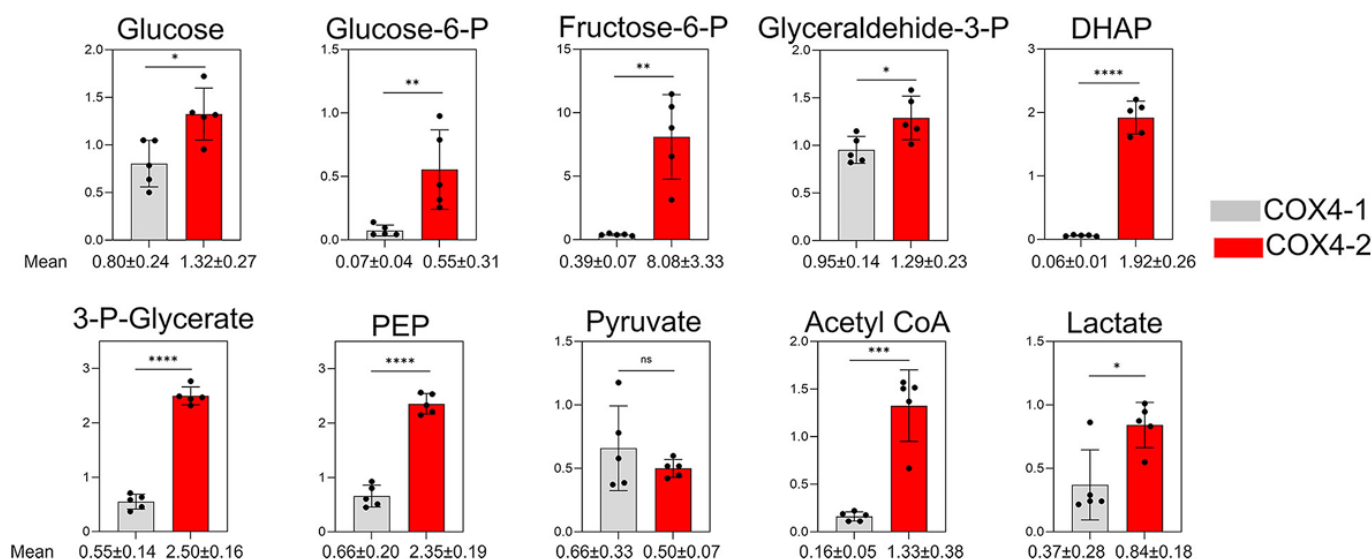


Figure 10: Effects of COX4 isoform expression on glycolysis metabolites in glioma cells under hypoxia. Bars represent the levels of key metabolites involved in the glycolytic pathway analyzed in COX4-1-expressing (gray bars) and COX4-2-expressing (red bars) glioma cells cultured under hypoxia for 24 hours. The numbers below each graph indicate the mean value ± SD for each metabolite, based on five independent measurements. *, $p < 0.05$; **, $p < 0.01$; ***, $p < 0.001$; ****, $p < 0.0001$; ns, not significant.

Discussion

GBM tumors commonly exhibit intrinsic or acquired resistance to standard therapeutic modalities, including chemotherapy and radiotherapy, and the hypoxic environment of these tumors exacerbates tumor growth, progression, and the resistance to treatment [28-30]. Additionally, hypoxia supports the maintenance of GBM stem cell populations, which are inherently resistant to standard treatments [31, 32]. This study reveals that expression of the CcO regulatory subunit isoform COX4-1 enhances GBM cell survival, proliferation, and radio resistance under hypoxic conditions.

Our previous studies underscore the significance and clinical implications of COX4-1 expression in GBM. We demonstrated a marked difference in OS between patients with tumors exhibiting high versus low COX4-1 expression. The median OS for patients with low COX4-1 expression was 22.18 months, compared to only 5.43 months for those with high COX4-1 expression. Additionally, our research revealed that COX4-1 plays a critical role in regulating glioma cancer cells' capacity for self-renewal and tumorigenicity [15]. Recent studies have also identified COX4-1 as essential for cell survival, proliferation, and in vivo progression of acute myeloid leukemia. Analysis of consortium databases further revealed pronounced COX4-1 expression and gene dependency in blood cancers, while COX4-2 expression remained undetectable [33]. These studies highlight the critical role of COX4-1 in maintaining mitochondrial homeostasis and suggest that targeting COX4-1 could have broad therapeutic potential, opening avenues for novel treatments across multiple cancer types.

Although glioma cells typically rely on glycolysis for energy, our previous studies showed that glioma cells expressing COX4-1 isoform, exhibit an increased reliance on OXPHOS under normoxic conditions [9, 15, 16, 21, 22]. The effects of this metabolic change in the context of hypoxia remained unknown, however. Our assessment of mitochondrial OCR, ATP production rate, glucose consumption, and lactate production in glioma cells in this study indicated that COX4-1 expression also prevents the hypoxia-induced downregulation of OXPHOS, and upregulation of glycolysis observed in COX4-2-expressing glioma cells. The COX4-1-dependent upregulation of OXPHOS was mediated by increased activity of each mitochondrial ETC complex. However, the maintenance of CcO activity in the context of hypoxia was particularly notable, as the activity of this complex, which links mitochondrial respiration to ATP production, was uniquely downregulated by hypoxia in COX4-2-expressing cells. Accordingly, the production of ATP increased only in the COX4-1-expressing cells upon exposure to hypoxia. This increase in energy production likely sustained the accelerated proliferation of the COX4-1-expressing cells observed under hypoxia in vitro and in the orthotopic mouse models of GBM.

However, despite the COX4-1-induced increase in the activity of complexes I and III, which are the major sources of mitochondrial $O_2^{\cdot-}$ production [34, 35], mitochondrial $O_2^{\cdot-}$ production was drastically lower in COX4-1-expressing glioma cells than in COX4-2-expressing cells. Furthermore, COX4-1 expression prevented the hypoxia-induced increase in mitochondrial $O_2^{\cdot-}$ production observed in COX4-2-expressing cells. Several publications have now shown that the assembly of mitochondrial complexes into SCs enhances the efficiency of electron transport through the ETC, thus minimizing ROS production while enhancing OXPHOS [9, 36-39]. We previously confirmed that COX4-1 expression triggers SC assembly in glioma cells [9]. The maintenance of these COX4-1-induced SCs observed under hypoxia in this study suggests that SC assembly is also responsible for the enhanced survival and proliferation of COX4-1-expressing glioma cells in hypoxic tumors.

Although the reliance on OXPHOS in a low-oxygen environment seems counterintuitive, similar findings have been reported in other cancer cells. For example, Ikeda et al. [10, 40] recently demonstrated in breast and endometrial cancer cells that overexpression of COX7RP, a CcO subunit that functions as an assembly factor of mitochondrial SC, promotes in vitro and in vivo growth, stabilizes mitochondrial SC assembly in hypoxic conditions, and increases hypoxia tolerance. Similarly, it was recently reported that SC assembly in pancreatic cancer cells maintains intact ETC functionality under hypoxia and SCs promote pancreatic cancer cell growth in hypoxia both in vitro and in vivo [20]. Additionally, COX6B2 was found to enhance CcO activity, increase OXPHOS, and facilitate SC assembly in lung adenocarcinoma cells, which enhanced the growth and proliferation of these cells under hypoxia [8]. These results highlight a crucial metabolic pathway that enables some cancer cells to thrive despite low oxygen levels and suggest potential targets for therapeutic intervention.

In addition to promoting the overall survival and proliferation of glioma cells under hypoxic conditions, COX4-1 expression exacerbated the hypoxia-induced radioresistance of these tumor cells upon re-exposure to ionizing radiation. This effect was likely mediated in part by the assembly of mitochondrial SCs, which substantially reduced the production of $O_2^{\cdot-}$ that would otherwise promote cell damage. Supporting this possibility, Lopez-Fabuel et al. observed that the high abundance of free complex I in the mitochondria of astrocytes correlated with increased ROS production compared with that in neurons, in which complex I was found predominately in SCs [38]. Furthermore, COX4-1 expression increased the mitochondrial reserve capacity, a measure of the ability of cells to resist oxidative stress [26], suggesting another mechanism by which these cells could resist the normally damaging effects of hypoxia and ionizing radiation.

Untargeted metabolomic analysis under hypoxia indicated that COX4-1 expression affects the steady-state levels of purine and methionine pathway intermediates, consistent with findings that purine synthesis contributes to aggressive behavior and therapy resistance in GBM [41, 42]. For instance, brain tumor-initiating cells activate de novo purine synthesis to maintain self-renewal and proliferation, which is associated with therapy resistance and tumor recurrence [41, 42]. In addition, abundance of the purinosome, the multi-enzyme complex responsible for de novo purine synthesis, is upregulated in response to low-oxygen environments [43]. Several reports have also suggested the malignant transformation or recurrence of GBM is associated with increased methionine [44, 45]. Methionine is crucial for cell growth and supports various cellular activities through its role in the folate cycle and as a methyl donor in the form of S-adenosylmethionine. Our results suggest that methionine metabolism and de novo purine synthesis in glioma cells expressing COX4-1 and containing SCs contribute to the increased hypoxia tolerance and resistance to ionizing radiation.

Conclusion

We conclude that COX4-1 enhances mitochondrial respiration, promotes SC assembly, reduces $O_2^{\cdot -}$ production, and increases resistance to ionizing radiation during hypoxia. These insights suggest that COX4-1 could be a valuable therapeutic target in radioresistant glioma cells in hypoxic tumors. Future research should explore the broader implications of COX4-1 expression and SC assembly in different cancer types and evaluate potential therapeutic strategies that target these pathways to overcome hypoxia-induced therapy resistance.

Acknowledgments: We wish to thank Dr. Erin Thacker for manuscript editing. The data presented herein were obtained at the Flow Cytometry Facility, which is a Holden Comprehensive Cancer Center core research facility at the University of Iowa.

Funding: This research was funded by the National Institute of Neurological Disorders and Stroke (NINDS) of the National Institutes of Health (NIH) under award number R01NS129702.

Ethics Statement

Animal Studies: The animal study protocol was approved by the Office of the Institutional Animal Care and Use Committee (IACUC protocol number 3032525-003).

Informed Consent Statement: N/A

Registry and the Registration No. of the study/trial: N/A.

Conflicts of Interest: The authors declare no conflicts of interest. The authors of this manuscript are not current Editor or Editorial Board Member of Cancer Science.

References

1. Carlos-Reyes A, Muniz-Lino MA, Romero-Garcia S, Lopez-Camarillo C, Hernandez-de la Cruz ON (2021) Biological Adaptations of Tumor Cells to Radiation Therapy. *Front Oncol* 11:718636.
2. Grasso D, Medeiros HCD, Zampieri LX, et al. (2020) Fitter Mitochondria Are Associated With Radioresistance in Human Head and Neck SQD9 Cancer Cells. *Front Pharmacol* 11:263.
3. Lynam-Lennon N, Maher SG, Maguire A, et al. (2014) Altered mitochondrial function and energy metabolism is associated with a radioresistant phenotype in oesophageal adenocarcinoma. *PLoS One* 9: e100738.
4. Morandi A, Indraccolo S (2017) Linking metabolic reprogramming to therapy resistance in cancer. *Biochim Biophys Acta Rev Cancer* 1868: 1-6.
5. Chedeville AL, Madureira PA (2021) The Role of Hypoxia in Glioblastoma Radiotherapy Resistance. *Cancers* 13:542.
6. Colwell N, Larion M, Giles AJ, et al. (2017) Hypoxia in the glioblastoma microenvironment: shaping the phenotype of cancer stem-like cells. *Neuro Oncol* 19:887-896.
7. Yang L, Lin C, Wang L, Guo H, Wang X (2012) Hypoxia and hypoxia-inducible factors in glioblastoma multiforme progression and therapeutic implications. *Exp Cell Res* 318:2417-2426.
8. Cheng CC, Wooten J, Gibbs ZA, McGlynn K, Mishra P, et al. (2020) Sperm-specific COX6B2 enhances oxidative phosphorylation, proliferation, and survival in human lung adenocarcinoma. *Elife* 9:e58108.
9. Oliva CR, Ali MY, Flor S, Griguer CE (2022) COX4-1 promotes mitochondrial supercomplex assembly and limits reactive oxygen species production in radioresistant GBM. *Cell Stress* 6:45-60.
10. Ikeda K, Horie-Inoue K, Suzuki T, et al. (2019) Mitochondrial supercomplex assembly promotes breast and endometrial tumorigenesis by metabolic alterations and enhanced hypoxia tolerance. *Nat Commun* 10:4108.
11. Vlasi E, Lagadec C, Vergnes L, et al. (2014) Metabolic differences in breast cancer stem cells and differentiated progeny. *Breast Cancer Res Treat* 146:525-534.
12. Grossman LI, Lomax MI (1997) Nuclear genes for cytochrome c oxidase. *Biochim Biophys Acta* 1352:174-192.
13. Huttemann M, Kadenbach B, Grossman LI (2001) Mammalian subunit IV isoforms of cytochrome c oxidase. *Gene* 267:111-123.
14. Pierron D, Wildman DE, Huttemann M, Markondapatnaikuni GC, Aras S, et al. (2012) Cytochrome c oxidase: evolution of control via nuclear subunit addition. *Biochim Biophys Acta* 1817:590-597.
15. Oliva CR, Markert T, Gillespie GY, Griguer CE (2015) Nuclear-encoded cytochrome c oxidase subunit 4 regulates BMI1 expression and determines proliferative capacity of high-grade gliomas. *Oncotarget* 6:4330-4344.
16. Oliva CR, Nozell SE, Diers A, et al. (2010) Acquisition of temozolomide chemoresistance in gliomas leads to remodeling of mitochondrial electron transport chain. *J Biol Chem* 285:39759-39767.
17. Fiorillo M, Ozsvari B, Sotgia F, Lisanti MP (2021) High ATP Production Fuels Cancer Drug Resistance and Metastasis: Implications for Mitochondrial ATP Depletion Therapy. *Front Oncol* 11:740720.
18. Cunatova K, Reguera DP, Vrbicky M, et al. (2021) Loss of COX41 Leads to Combined Respiratory Chain Deficiency and Impaired Mitochondrial Protein Synthesis. *Cells* 10:369.

19. Pajuelo Reguera D, Cunatova K, Vrbacky M, et al. (2020) Cytochrome c Oxidase Subunit 4 Isoform Exchange Results in Modulation of Oxygen Affinity. *Cells* 9:443.
20. Hollinshead KER, Parker SJ, Eapen VV, et al. (2020) Respiratory Supercomplexes Promote Mitochondrial Efficiency and Growth in Severely Hypoxic Pancreatic Cancer. *Cell Rep* 33:108231.
21. Oliva CR, Ali MY, Flor S, Griguer CE (2022) Effect of Expression of Nuclear-Encoded Cytochrome C Oxidase Subunit 4 Isoforms on Metabolic Profiles of Glioma Cells. *Metabolites* 12:748.
22. Oliva CR, Moellering DR, Gillespie GY, Griguer CE (2011) Acquisition of chemoresistance in gliomas is associated with increased mitochondrial coupling and decreased ROS production. *PLoS One* 6:e24665.
23. Flor S, Oliva CR, Ali MY, et al. (2021) Catalase Overexpression Drives an Aggressive Phenotype in Glioblastoma. *Antioxidants (Basel)* 10:1988.
24. Ali MY, Oliva CR, Flor S, Goswami PC, Griguer CE (2022) Cytochrome c oxidase mediates labile iron level and radioresistance in glioblastoma. *Free Radic Biol Med* 185:25-35.
25. Hill BG, Benavides GA, Lancaster JR, et al. (2012) Integration of cellular bioenergetics with mitochondrial quality control and autophagy. *Biol Chem* 393:1485-1512.
26. Hill BG, Dranka BP, Zou L, Chatham JC, Darley-Usmar VM (2009) Importance of the bioenergetic reserve capacity in response to cardiomyocyte stress induced by 4-hydroxynonenal. *Biochem J* 424:99-107.
27. Matsui T, Nuryadi E, Komatsu S, et al. (2019) Robustness of Clonogenic Assays as a Biomarker for Cancer Cell Radiosensitivity. *Int J Mol Sci* 20:4148.
28. Griguer CE, Oliva CR (2011) Bioenergetics pathways and therapeutic resistance in gliomas: emerging role of mitochondria. *Curr Pharm Des* 17:2421-2427.
29. Kaur B, Khwaja FW, Severson EA, Matheny SL, Brat DJ, et al. (2005) Hypoxia and the hypoxia-inducible-factor pathway in glioma growth and angiogenesis. *Neuro Oncol* 7:134-153.
30. Vlashi E, Lagadec C, Vergnes L, et al. (2011) Metabolic state of glioma stem cells and nontumorigenic cells. *Proc Natl Acad Sci U S A* 108:16062-16067.
31. Auffinger B, Spencer D, Pytel P, Ahmed AU, Lesniak MS (2015) The role of glioma stem cells in chemotherapy resistance and glioblastoma multiforme recurrence. *Expert Rev Neurother* 15:741-752.
32. Bao S, Wu Q, McLendon RE, et al. (2006) Glioma stem cells promote radioresistance by preferential activation of the DNA damage response. *Nature* 444:756-760.
33. Zhang L, Zhang H, Wang TY, et al. (2024) Nuclear Control of Mitochondrial Homeostasis and Venetoclax Efficacy in AML via COX4I1. *Adv Sci (Weinh)* 12:e2404620.
34. Bleier L, Droese S (2013) Superoxide generation by complex III: from mechanistic rationales to functional consequences. *Biochim Biophys Acta* 1827:1320-1331.
35. Brand MD. The sites and topology of mitochondrial superoxide production. *Exp Gerontol* 45:466-472.
36. Lapuente-Brun E, Moreno-Loshuertos R, Acin-Perez R, et al. (2013) Supercomplex assembly determines electron flux in the mitochondrial electron transport chain. *Science* 340:1567-1570.
37. Lenaz G, Tioli G, Falasca AI, Genova ML (2016) Complex I function in mitochondrial supercomplexes. *Biochim Biophys Acta* 1857:991-1000.
38. Lopez-Fabuel I, Le Douce J, Logan A, et al. (2016) Complex I assembly into supercomplexes determines differential mitochondrial ROS production in neurons and astrocytes. *Proc Natl Acad Sci U S A* 113:13063-13068.
39. Maranzana E, Barbero G, Falasca AI, Lenaz G, Genova ML (2013) Mitochondrial respiratory supercomplex association limits production of reactive oxygen species from complex I. *Antioxid Redox Signal* 19:1469-1480.
40. Ikeda K, Shiba S, Horie-Inoue K, Shimokata K, Inoue S (2013) A stabilizing factor for mitochondrial respiratory supercomplex assembly regulates energy metabolism in muscle. *Nat Commun* 4:2147.
41. Zhou W, Wahl DR (2020) Purine metabolism promotes radioresistance and is a therapeutic target in glioblastoma. *Mol Cell Oncol* 7:1834902.
42. Zhou W, Yao Y, Scott AJ, et al. (2020) Purine metabolism regulates DNA repair and therapy resistance in glioblastoma. *Nat Commun* 11:3811.
43. Doigneaux C, Pedley AM, Mistry IN, Papayova M, Benkovic SJ, et al. (2020) Hypoxia drives the assembly of the multienzyme purinosome complex. *J Biol Chem* 295:9551-9566.
44. Sowers ML, Sowers LC (2022) Glioblastoma and Methionine Addiction. *Int J Mol Sci* 23:7156.
45. Zhou S, Zhao X, Zhang S, et al. (2023) Prognosis prediction based on methionine metabolism genes signature in gliomas. *BMC Med Genomics* 16:317.